Talanta 110 (2013) 135–143

Contents lists available at SciVerse ScienceDirect

Talanta

journal homepage: www.elsevier.com/locate/talanta

Green synthesized nickel nanoparticles modified electrode in ionic liquid medium and its application towards determination of biomolecules

Rajendran Suresh Babu, Pandurangan Prabhu, Sangilimuthu Sriman Narayanan*

Department of Analytical Chemistry, School of Chemical Sciences, University of Madras, Guindy Campus, Chennai 600 025, Tamil Nadu, India

ARTICLE INFO

Article history:
Received 23 November 2012
Received in revised form
8 February 2013
Accepted 12 February 2013
Available online 5 March 2013

Keywords:
Room temperature ionic liquid
1-ethyl-3-methylimidazolium ethyl sulfate
Amperometric sensor
Cyclic voltammetry
Nickel nanoparticles

ABSTRACT

An air and moisture stable ionic liquid 1-ethyl-3-methylimidazolium ethyl sulfate (EMIMES) was used as an electrolyte for electropolymerization of L-cysteine followed by electrodeposition of nickel nanoparticles (NiNP) on paraffin wax impregnated graphite electrode (PIGE). The electrodeposited NiNP modified electrode showed good redox activity and stability in 0.1 M KOH solution. The modified electrode has been characterized using Fourier transform infrared spectroscopy (FTIR), Raman spectroscopy, X-ray photoelectron spectroscopy (XPS), field emission scanning electron microscopy (FESEM), energy dispersive X-ray spectroscopy (EDS), electrochemical impedance spectroscopy (EIS) and cyclic voltammetry (CV). The modified electrode was examined for electrocatalytic oxidation of some compounds of biological and clinical importance such as vitamin B_6, L-tyrosine, L-tryptophan, vanillin, glucose and hydrogen peroxide by cyclic voltammetry to demonstrate the electrocatalytic activity of the electrodeposited NiNPs.

1. Introduction

Room-temperature ionic liquids (RTILs) are materials that are composed entirely of ions and are liquids below 100 °C [1]. The unique properties of RTILs make them particularly promising for electrochemical applications. RTILs are ionically conductive and hence electrochemistry can be performed using RTILs as supporting electrolytes. Many RTILs offer wide potential windows (the potential range over which the RTIL is electrochemically inert), thermal and chemical stability, very low vapor pressures, and the ability to dissolve a wide range of chemical species. Due to the unique combination of these properties, electrochemists have proposed the use of RTILs in a wide range of devices including photoelectrochemical cells [2], supercapacitors [3], fuel cells [4], batteries [5] and electrochemical sensors [6,7]. Modified electrodes offer higher selectivity, sensitivity, greater time efficiency and higher stability than the conventional electrodes. Therefore, several modifiers such as polymers [8–11], DNA doped polymers [12], dye doped sol–gels [13], metal oxides [14], carbon nanotubes [15,16], inorganic redox mediators [17] and metal nanoparticles (MNPs) [18–20] have been used to fabricate modified electrodes. Among them, MNPs modified electrodes have drawn particular attention due to their high surface area, effective mass transport, catalysis and control over local microenvironment compared to electrodes modified with macroparticles [21,22]. However, the MNPs at the electrode surface can be fragile in the absence of stabilizing conductive material. To address this problem, the electrode surface can be modified with some conductive stabilizing materials such as carbon nanotubes and polymers [23,24] and then the MNPs can be attached to the modified electrode surface. Moreover, the porous nature of conducting polymer allows dispersing of the metal nanoparticles into the polymer matrix and generates additional electrocatalytic sites [25–27]. Polycysteine (PC) is one of the important polyaminoacid, its structure is relevant to biopolymers and it supports the metal nanoparticles. Platinum nanoparticles–polypyrrole modified electrodes have been employed to determine nitrite and to study proton and oxygen reduction [28,29]. To the best of our knowledge, there is no reported relevant literature available for the determination of biologically and clinically important compounds at polycysteine functionalized nickel nanoparticles (PCFNiNP) modified electrodes.

In the present study, a modified electrode was prepared by electrochemical deposition of NiNP in over-oxidized polycysteine film modified graphite electrode in ionic liquid medium and the performance of the electrode was studied by cyclic voltammetry and surface examination was made using FESEM. The PCFNiNP modified electrode was used as the sensing matrix for the determination of vitamin B_6, L-tyrosine, L-tryptophan, vanillin, glucose and hydrogen peroxide at micromolar levels.

2. Experimental

2.1. Reagents

Vitamin B_6, L-tryptophan, L-tyrosine, D-glucose, vanillin and hydrogen peroxide were purchased from HIMEDIA and dissolved

* Corresponding author. Tel.: +91 44 22202717; fax: +91 44 22352494.
E-mail addresses: sriman55@yahoo.com, sriman55@gmail.com (S. Sriman Narayanan).

0039-9140/$ - see front matter © 2013 Elsevier B.V. All rights reserved.
http://dx.doi.org/10.1016/j.talanta.2013.02.025

before use. All other chemicals used in this investigation were of analytical grade. EMIMES (purity 98.5%) was obtained from Alfa Aesar, spectroscopic grade graphite rod (3 mm diameter) was used as received from Aldrich. Double distilled water employed in all experiments was obtained from a Millipore-Milli-Q system.

2.2. Apparatus and measurements

FTIR spectra were recorded using a Perkin–Elmer RX 1 spectrometer. Raman spectra were recorded with Raman 11i system (Nanophoton Corp., Japan). For the study of morphology and chemical composition of the PCFNiNP modified electrode, FE-SEM and EDS data were obtained on a SU6600 field emission scanning electron microscopy (FE-SEM) (HITACHI, Japan), equipped with an energy-dispersive X-ray analyzer at an accelerating voltage of 30 kV. XPS measurement for surface analysis was performed on a monochromatic 300 W Al Kα X-ray radiation as the X-ray source for excitation (Model XM 1000, Omicron Nanotechnology, Germany).

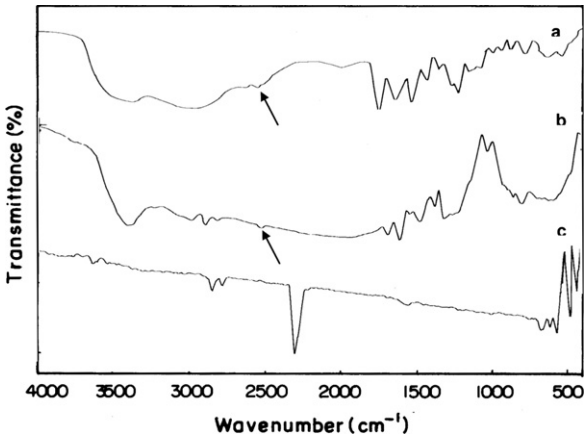

Fig. 1. FTIR spectrum of pure (a) L-cysteine, (b) PC modified electrode and (c) PCFNiNP modified electrode.

Electrochemical measurements were performed with a CHI 660B electrochemical workstation (CH Instruments, USA) controlled by a personnel computer. Three electrode system was employed for this study. A platinum wire and a saturated calomel electrode (SCE) were used as auxiliary and reference electrodes, respectively. All potentials were referred to the latter. The modified electrode employed as the working electrode was prepared according to the procedure described below. A magnetic Teflon stirrer provided the convective transport during the amperometric measurements. All electrochemical experiments were performed in 0.1 M KOH solutions.

2.3. Construction of the PCFNiNP modified electrode

PIGE with a circular surface diameter of 3 mm prepared as reported [30] was used for electrode modification. One end of the electrode was carefully polished on a smooth surface and with 0.5 μm alumina, washed with distilled water and dried in air. Then, the polished surface was used for electrode modification. The electropolymerization of 0.01 M L-cysteine was carried out in 0.1 M EMIMES by cycling the potential between −0.6 to 2.0 V at 50 mV/s scan rate. A thin polycysteine (PC) formed with 15 deposition cycles was used in all experiments. After removing the electrode from depositing solution, it was washed with ultrapure

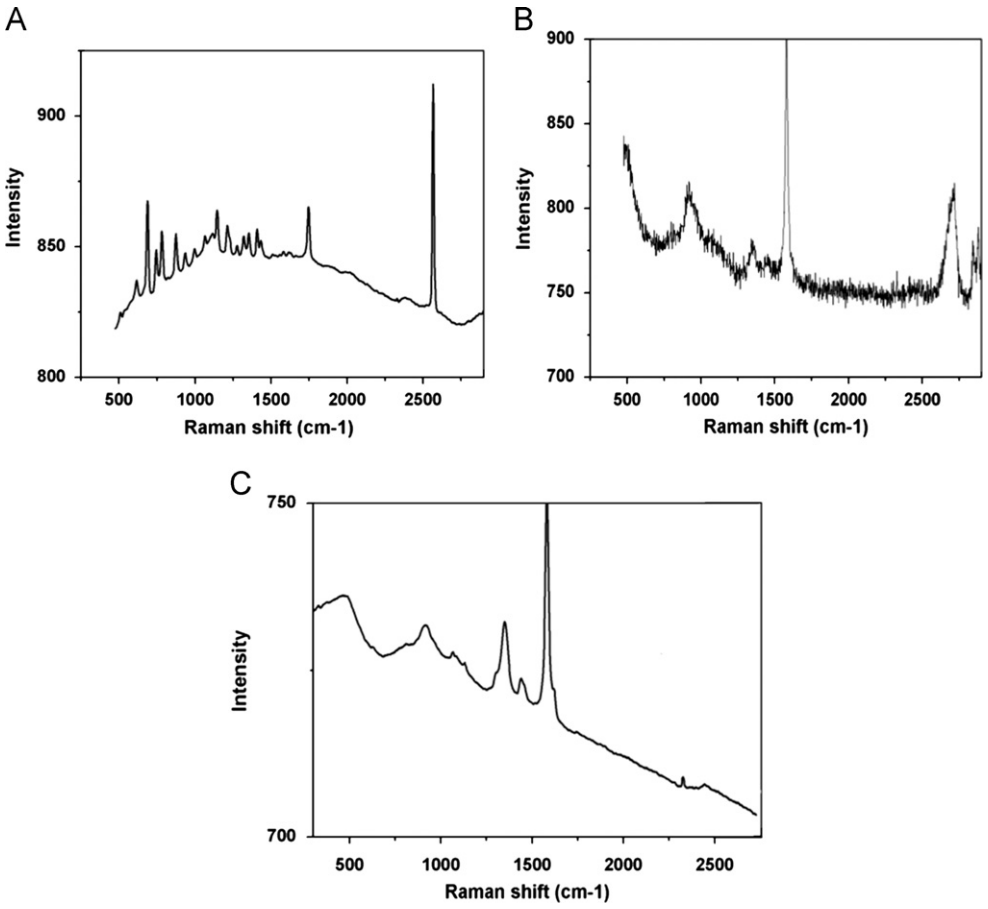

Fig. 2. Raman spectra of (A) pure L-cysteine, (B) PC modified electrode and (C) PCFNiNP modified electrode.

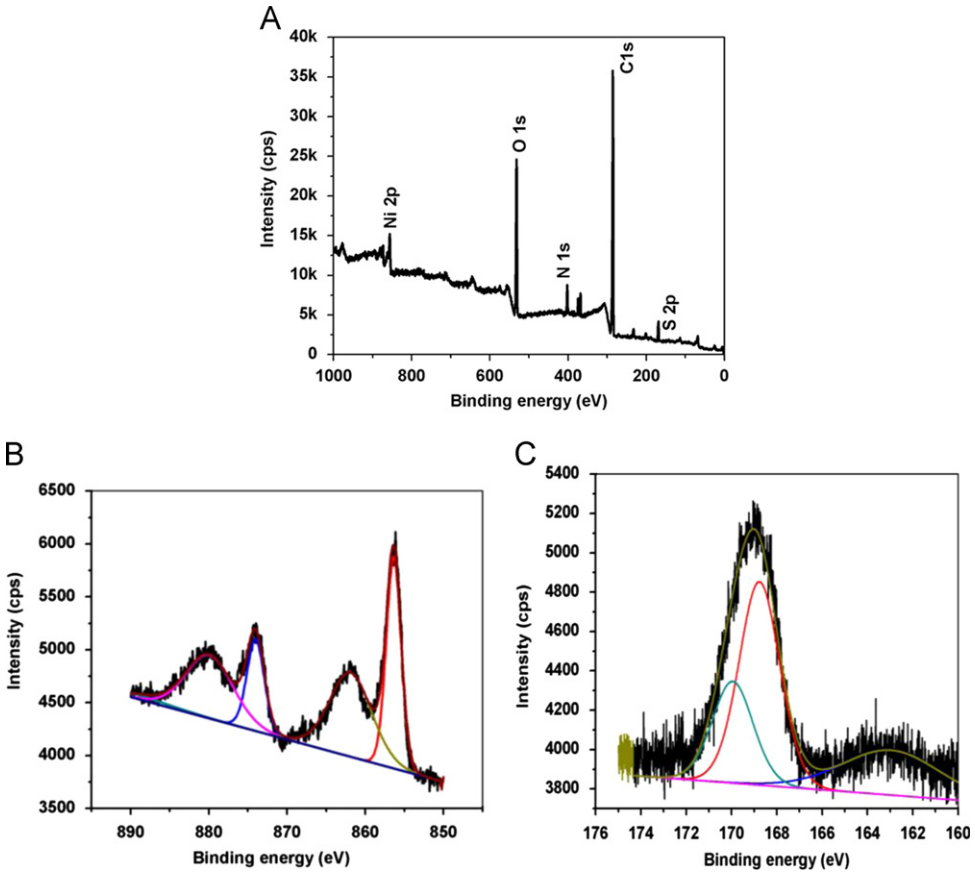

Fig. 3. XPS spectra of (A) Survey spectra (B) Ni2p core (C) S2p core of the PCFNiNP modified electrode.

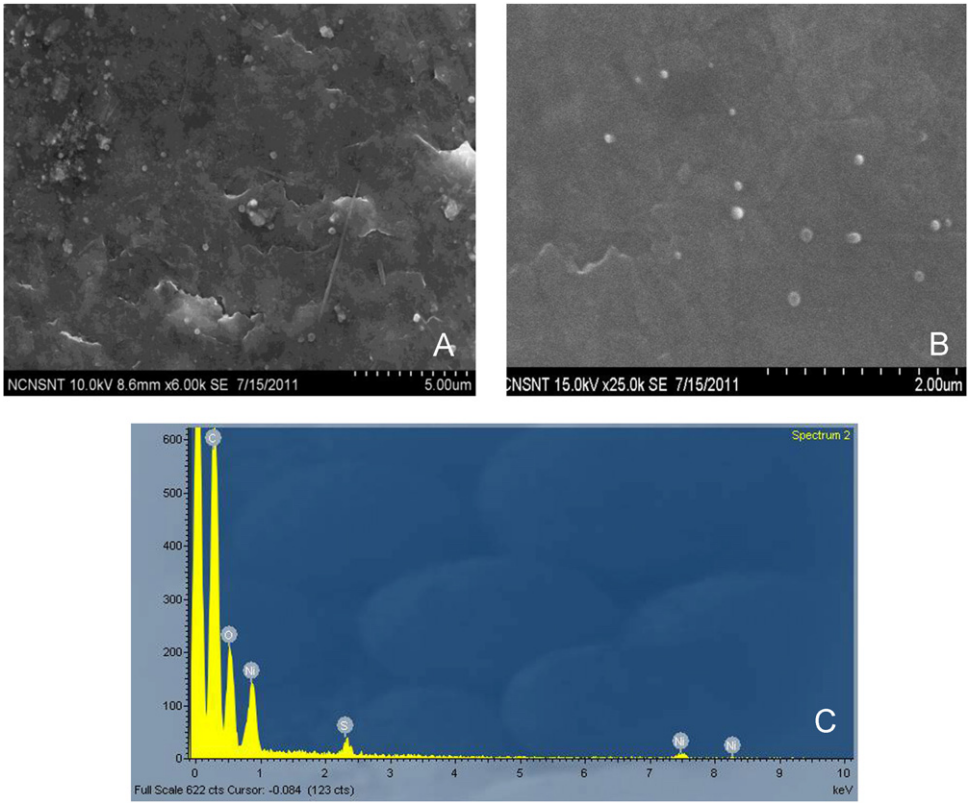

Fig. 4. FESEM images of (A) PCFNiNP modified electrode with 6 kx magnificent, (B) PCFNiNP modified electrode with 25 kx magnificent and (C) EDS spectrum of the PCFNiNP modified electrode.

water to remove the unbound materials remaining on the electrode surface.

2.4. NiNPs deposition

NiNPs were deposited electrochemically on the PC modified PIGE in a solution containing 0.1 mM $NiSO_4$ and 0.1 M EMIMES under a constant potential of −1.2 V for 100 s. After the modification with NiNPs, the electrode was thoroughly washed to remove the excess materials from the electrode surface and then dried at room temperature.

3. Results and discussion

3.1. FTIR-ATR spectroscopy

The FTIR study of the PCFNiNP modified electrode was conducted in the reflection mode and the results are shown in Fig. 1. The FTIR spectra of crystalline L-cysteine (curve a), electropolymerized L-cysteine (PC) (curve b) and PCFNiNP (curve c) are shown. On comparing the three curves, the most important difference noticed between them is the band at 2553 cm^{-1} corresponding to the thiol (–SH) group which is present only in curve a and curve b. In the case of PCFNiNP modified electrode the peak at 2553 cm^{-1} has disappeared. The disappearance of peak is attributed to the cleavage of S–H bond and the formation of S–Ni bond which is in confirmation with the XPS study [31]. The peak at 476 and 432 cm^{-1} confirms the formation of Ni–S bond [32]. Based on the above results it seems that only the thiol group is involved in the bonding with the NiNP.

3.2. Raman spectroscopy

The Raman spectra of pure L-cysteine (A), PC (B) and PCFNiNP (C) are shown in Fig. 2. The Raman spectrum of L-cysteine and PC modified electrode show absorption at 2565 cm^{-1} which indicates the presence of free –SH group in L-cysteine and PC modified electrode. The absence of a peak at this position for the PCFNiNP modified electrode confirms the absence of free –SH group in the above electrode. The absorption at 1579 cm^{-1} corresponds to NH_3^+ symmetrical deformation and is present in PC modified electrode as well as PCFNiNP modified electrode indicating the presence of PC in both electrodes. The peak at 471 cm^{-1} confirms the formation of Ni–S bond. These observations are in consistent with earlier report [33].

3.3. X-ray photoelectron spectroscopy

To give further evidence that nickel is present on the PC modified electrode, XPS experiments have been carried out. Fig. 3 shows the XPS survey spectrum and high resolution XPS spectrum of S (2p) and Ni (2p) respectively for the PCFNiNP modified electrode. The peaks at 855.6 and 873.3 eV correspond to the binding energies of Ni ($2p_{3/2}$) and Ni ($2p_{1/2}$) respectively, which is consistent to the reported value for NiS [31,34]. Two strong satellite peaks at 861.1 and 879.2 eV corresponds to Ni ($2p_{3/2}$) and Ni ($2p_{1/2}$) were also observed. The binding energy of S (2p) at 162.5 eV is also in good agreement with that reported in the literature [35,36]. The fact that NiNP was shown to be functionalized onto the polycysteine electrode surface opens up new possibilities for further investigations particularly for the oxidation of biomolecules through nickel in the PCFNiNP modified electrode.

3.4. FESEM analysis

The modified electrodes were characterized also by FESEM. The use of RTILs (EMIMES) with the imidazolium ion leads to low interfacial tensions, but the nucleation rate is higher than in conventional solvents due to the higher conductivity and viscosity of ionic liquids. Fig. 4A and B shows the formation of the NiNPs on the electrode surface, and its size ranges between 100 and 200 nm. The particles were distributed almost evenly over the electrode surface. The particle size surely plays a vital role in the electrochemical characteristics of the modified electrode. The electrochemical response of modified electrode was enhanced which could be due to the high surface area provided by the nanoparticle. To identify the elemental composition of the PCFNiNP modified electrode, EDS measurement was carried out. The corresponding result is shown in Fig. 4C. The peaks appearing at 0.8, 7.5 and 8.3 keV are related to Ni, and the other peak at 2.4 keV corresponds to S. Fig. 4C reveals that the PCFNiNP modified electrode is composed of C, O, S and Ni elements which are the elements present in the PCFNiNP modified electrode.

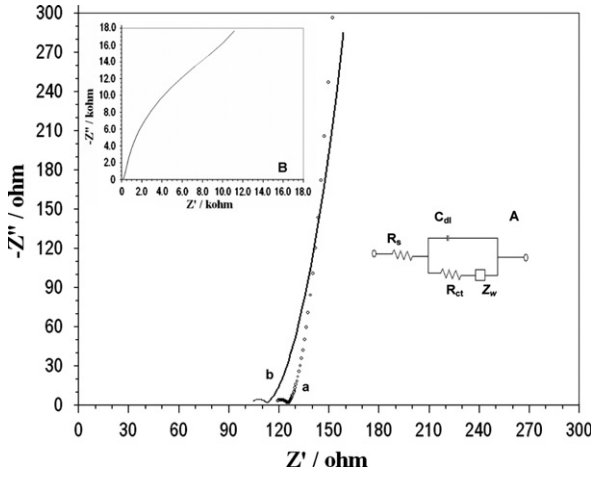

Fig. 5. EIS of (a) PC modified electrode and (b) PCFNiNP modified electrode in 10 mM. $K_4[Fe(CN)_6]$ in 0.1 M KCl solution, with the frequency swept from 1 Hz to 0.1 MHz. Inset: (A) modified Randles equivalent circuit diagram and (B) EIS of bare electrode.

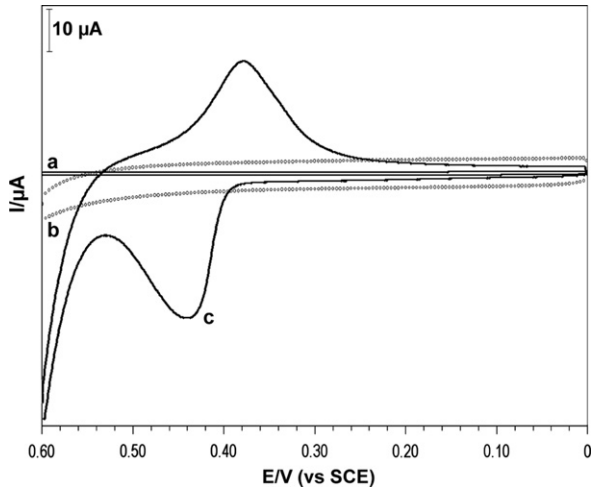

Fig. 6. Cyclic voltammograms of (a) bare electrode, (b) PC modified electrode and (c) PCFNiNP modified electrode in 0.1 M KOH; Scan rate: 50 mV/s.

3.5. Electrochemical impedance spectroscopy

EIS was employed to study the impedance changes of the electrode surface. By using $Fe(CN)_6^{3-/4-}$ redox couple as the electrochemical probe, the Nyquist plots of different electrodes were recorded as shown in Fig. 5 with the frequencies ranging from 1 Hz to 0.1 M Hz. In order to give more quantitative information, a modified Randles equivalent circuit was chosen to fit the measurement results (Inset **A**). At the bare electrode the electron-transfer resistance (R_{ct}) was estimated to be 8089 Ω (Inset B). The R_{ct} decreased dramatically to 8.271 Ω for PC modified electrode (curve a), indicating that the electrode containing PC form high electron conduction pathways between the electrode and electrolyte. The PCFNiNP modified electrode has shown 7.812 Ω as R_{ct} (curve b), which indicates the improved conducting in presence of NiNPs. The results indicated that NiNPs were successfully immobilized on the surface of the modified electrode.

3.6. Cyclic voltammetric studies of the PCFNiNP modified electrode

The electrochemical behavior of the PCFNiNP modified electrode was studied by cyclic voltammetry. Cyclic voltammetric investigations of the PCFNiNP modified electrode reveals (Fig. 6) a pair of peaks corresponding to the immobilized NiNP when the potential was swept in the range from 0 to 0.6 V at a scan rate of 50 mV/s in 0.1 M KOH (curve **c**). The anodic and cathodic peak potentials were observed at 0.44 V and 0.37 V respectively with a formal potential E^0 [$E^0=(E_{pa}+E_{pc})/2$] of 0.40 V, where E_{pa} and E_{pc} are the anodic and the cathodic peak potentials respectively. CV response for the bare electrode and PC modified electrode under similar condition did not show any characteristic wave (curves a and b). The electrochemical behavior of the PCFNiNP modified electrode in alkaline solution seems to be similar to that of pure Ni [37] and Ni–Cr [38] alloy electrode in the same solution, for which the redox system corresponding to these peaks was assigned to Ni(II)/Ni(III) couple which can be given as [39]

$$Ni(OH)_2 + OH^- \rightleftharpoons NiO(OH) + e^- + H_2O \quad (1)$$

3.7. Effect of scan rates

The effect of scan rate on the peak current of PCFNiNP modified electrode was examined. With increase in scan rates from 5 to 150 mV/s the currents for both peaks increased as shown in Fig. 7A. The anodic and cathodic peak currents are linearly proportional to the square root of the scan rate which is expected for a diffusion controlled electrode process, with correlation coefficients of 0.9965 and 0.9981 for anodic and cathodic peaks respectively (Fig. 7B). At higher scan rates (>200 mV/s), the peak currents were proportional to the scan rate indicative of a surface confined redox process, which indicated the limitation arising from charge transfer kinetics.

According to the method demonstrated by Laviron [40], the charge transfer coefficient, α, and the apparent heterogeneous charge transfer rate constant, k_s of a surface-confined redox couple can be estimated in cyclic voltammetry from the variation of the anodic and cathodic peak potentials as a function of the logarithm of scan rates. For higher scan rates, this theory predicts a linear dependence of E_p vs. log v, which can be used to extract the kinetic parameters of α and k_s from the slope and intercept of such plots, respectively. Fig. 7C, shows the variation of the peak potentials vs. the logarithm of the scan rate obtained from the cyclic voltammograms of the

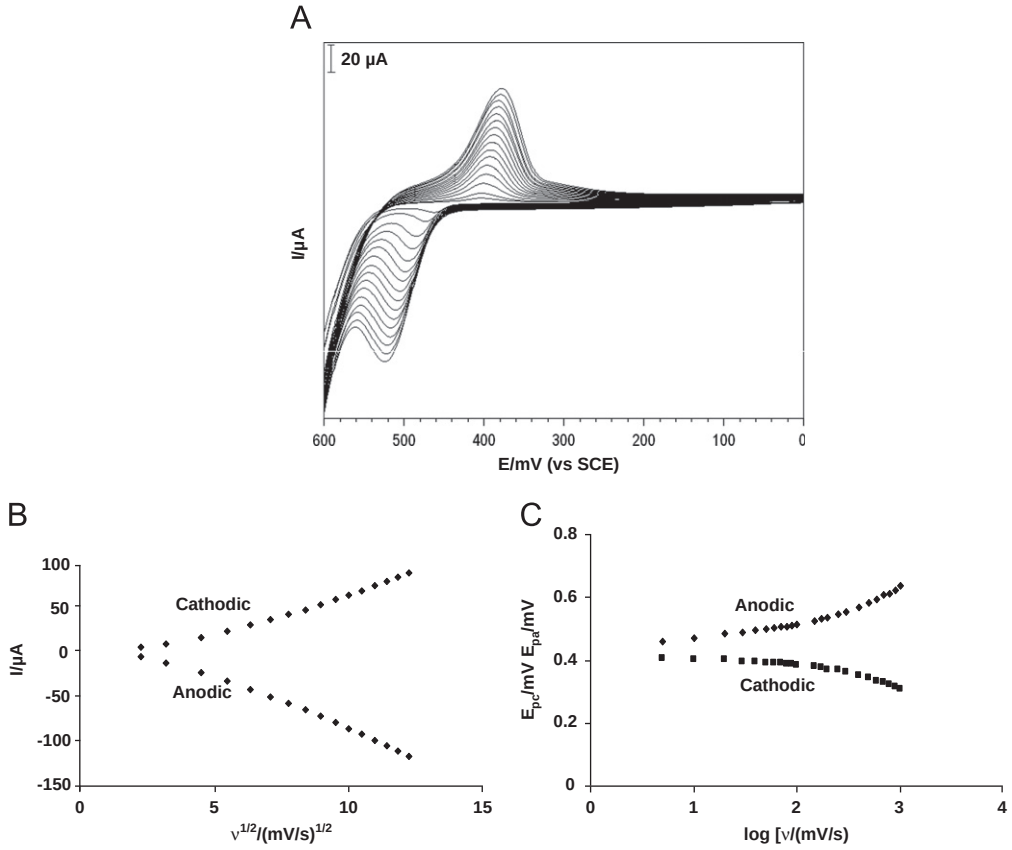

Fig. 7. (A) Cyclic voltammograms of the PCFNiNP modified electrode at different scan rates in 0.1 M KOH. The scan rates from 5 to 150 mV/s (inner to outer). (B) Dependence of peak current (I_{pa} and I_{pc}) vs. square root the scan rate ($\nu^{1/2}$) and (C) plot of the variation of peak potential vs. logarithm of the scan rates.

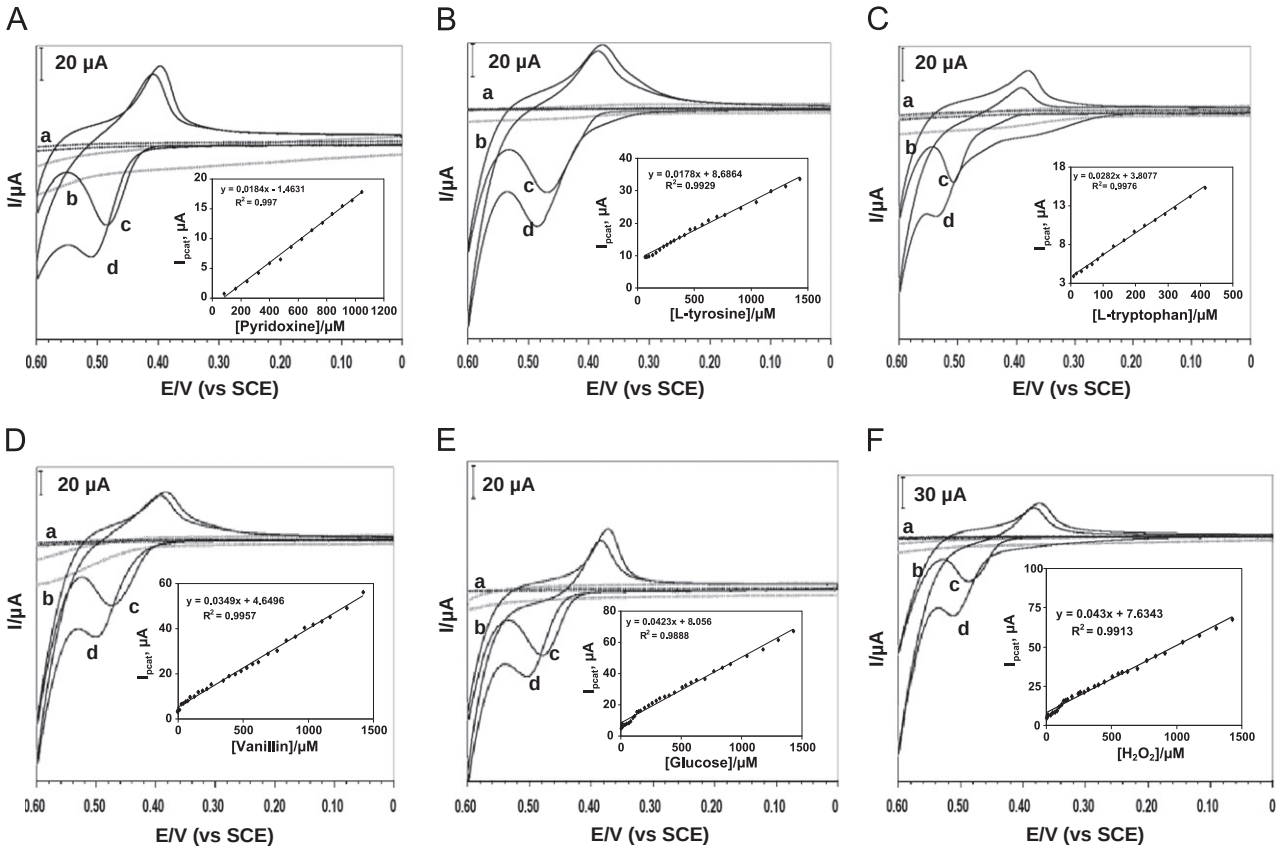

Fig. 8. Cyclic voltammograms for the electrocatalytic oxidation of: (A) vitamin B_6, (B) L-tyrosine, (C) L-tryptophan, (D) vanillin, (E) glucose and (F) H_2O_2; (a) and (b) bare electrode and PC modified electrode in the presence of 6.25×10^{-4} M analyte, (c) PCFNiNP modified electrode, and (d) PCFNiNP modified electrode in the presence of 6.25×10^{-4} M analyte.

Table 1
Results of analyte determination with the PCFNiNP modified electrode.

Analytes	Working potential (V)	Linear range (μM)	Limit of detection (μM) @ 0.50 V			Correlation coefficient	RSD for ten successive measurement (%)
			Bare	PC	PCFNiNP		
Vitamin B_6	0.50	8.3–1600	484.3	107.5	2.70	0.9902	2.1
L-Tyrosine	0.50	1.6–1400	476.1	158.7	0.53	0.9929	1.9
L-Tryptophan	0.54	8.3–1000	334.8	183.7	2.70	0.9976	2.4
Vanillin	0.50	3.3–1400	256.4	158.7	1.10	0.9957	2.7
Glucose	0.50	1.6–1400	333.3	256.4	0.53	0.9888	1.7
H_2O_2	0.50	3.3–1700	476.1	133.3	1.10	0.9913	1.8

Table 2
Comparison of the performance of the proposed PCFNiNP modified electrode with the reported methods.

Analytes	CME based on linear range (μM)	LOD (μM)	Sensitivity (μA/mM)	Ref.
L-Tryptophan				
TiO_2-GR/4-ABSA/GCE	1–400	0.3	0.2290	[42]
Ag/Rutin/WCE	0.7–70	0.1	–	[43]
PCFNiNP modified electrode	8.3–1000	2.7	28.2	[This work]
Glucose				
GOD-Chitosan-BDCNiNP	2.5–1190	8.3	0.25	[44]
CuNP/MWCNT	10–300	0.5	50.4	[45]
PCFNiNP modified electrode	1.6–1400	0.5	42.3	[This work]
H_2O_2				
MWCNT/AgNP–Au	50–1700	0.5	1.42	[46]
CuO nanorod bundles	100–800	0.2	150.0	[47]
PCFNiNP modified electrode	3.3–1700	1.1	43.0	[This work]

TiO_2-GR/4-ABSA/GCE—TiO_2-graphene/poly(4-aminobenzenesulfonic acid) GCE, Ag/Rutin/WCE—Silver nanoparticle/rutin/paraffin-impregnated graphite electrode, GOD-Chitosan-BDCNiNP—Glucose oxidase-chitosan-boron-doped carbon-coated NiNP, CuNP/MWCNT—Copper nanoparticle/Multiwalled carbon nanotube, MWCNT/AgNP–Au—multi-wall carbon nanotube/silver nanoparticle nanohybrids modified Au electrode.

modified electrode. It is found that the ΔE_p values are proportional to the logarithm of the scan rate, for the scan rates higher than 400 mV/s. A plot of E_p vs. log ν yields two straight lines with slopes of $2.3RT/(1-\alpha)nF$ for anodic and $-2.3RT/\alpha nF$ for the cathodic peak. The value of α was calculated to be 0.61. Laviron's equation can also be used to determine the electron transfer rate (k_s) between the NiNP and the electrode and from the value of ΔE_p corresponding to different scan rates, an average value of k_s was calculated to be 1.03 ($\pm$0.02) cm/s. The electrochemical rugosity (Γ) or surface concentration of the electroactive species was also estimated [41]. The Γ of the PCFNiNP modified electrode was calculated to be 1.902×10^{-8} mol/cm^2 at a scan rate of 20 mV/s.

Scheme 1. Mechanism for the electrocatalytic oxidation of analytes at the PCFNiNP modified electrode.

3.8. Electrocatalytic oxidation studies

The application of PCFNiNP modified electrode towards the electrocatalytic oxidation of some pharmaceutically and biologically significant compounds has been studied. The CVs of the bare electrode, PC modified electrode and the PCFNiNP modified

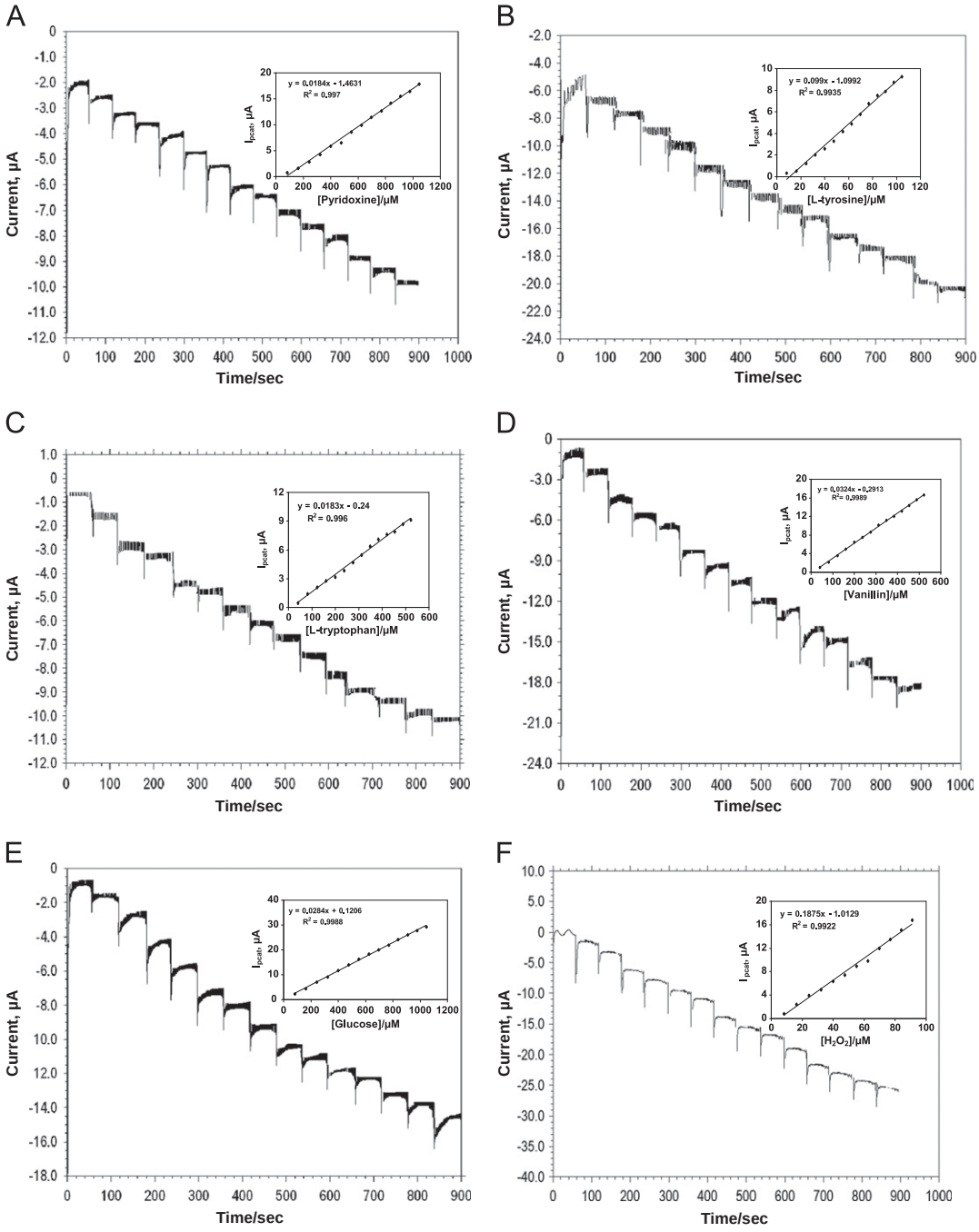

Fig. 9. Chronoamperometric response for the (A) vitamin B_6, (B) L-tyrosine, (C) L-tryptophan, (D) vanillin, (E) glucose and (F) H_2O_2 at the PCFNiNP modified electrode for each addition of 0.5 mL of 5 mM analyte to 0.1 M KOH solution; stirring rate 300 rpm, at fixed working potential. Inset: calibration graphs for analyte concentration.

electrode in presence and absence of 6.25×10^{-4} M vitamin B_6, L-tyrosine, L-tryptophan, vanillin, glucose and hydrogen peroxide are shown in Fig. 8. For the modified electrode an enhancement in anodic peak current appeared for the addition of 6.25×10^{-4} M of analytes indicating a strong electrocatalytic effect. The anodic wave for all the analytes starts at 0.44 V and anodic peak potential is about 0.54 V, while at the bare electrode the analytes are not oxidized in the potential range from 0 to 0.6 V. Similarly for the PC modified electrode, no distinct catalytic oxidation peak was observed for all the analytes even though a higher current was observed than the bare electrode. Furthermore, modified electrode gave a substantially higher sensitivity for all the analytes. As shown in the figures no detectable reduction peak was observed in the reverse scan, indicating that the electrochemically generated products cannot be reduced in the potential range studied.

The anodic peak current was found to increase with increase in analyte concentration in the solution. The plot of catalytic current vs. concentration of analytes is shown in insets of Fig. 8 for all the analytes. The linear range, correlation coefficient, detection limit, working potential and relative standard deviation (RSD) of the analytes determination at the proposed electrode are shown in Table 1. A good linear response was obtained for the wide concentration range of all these analytes. A comparison of the oxidation by the bare, PC modified and PCFNiNPs modified electrodes reveals that the PCFNiNPs modified electrodes exhibited enhanced catalytic current due to high surface area in the presence of NiNP attached in the protective PC surface which prevented the passive layer formation and the possible dissolution of the NiNP in the electrode surface. Combining the data obtained from the experiments, it can be concluded that the NiNP decorated PC has resulted in higher catalytic activity towards the oxidation of biomolecules and deserves to be a good electrochemical sensor. Table 2 shows the linear working range, limit of detection and sensitivity obtained with the present sensor along with some of the previously reported metallic nanoparticle modified electrodes for the determination of some of the common analytes. It is concluded that the proposed sensor is comparable to other reported sensors. The possible mechanism for the electrocatalytic oxidation of analytes is shown in Scheme 1.

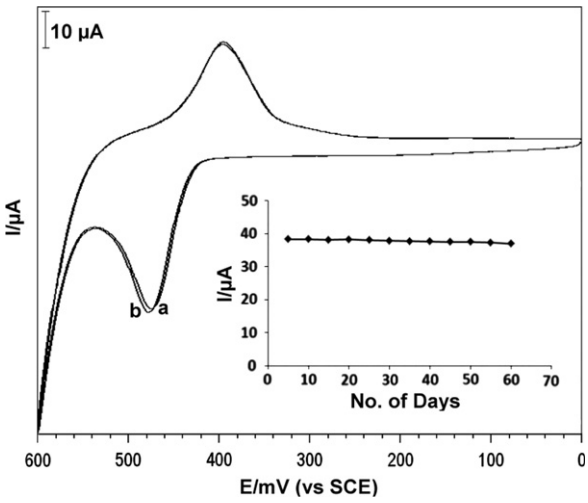

Fig. 10. Cyclic voltammograms of the (a) 1st and (b) 100th scan of the PCFNiNP modified. electrode in 0.1 M KOH; Scan rate: 50 mV/s. Inset. The long term stability plot of the PCFNiNP modified electrode.

3.9. Amperometric studies

Since the cyclic voltammetry is not particularly sensitive for low concentrations, experiments under stirred conditions or in flow medium was employed using amperometric method. In addition, the response time of the modified electrode in stirred solution was rapid (< 3 s). Therefore, amperometry was employed with a stirred solution to detect the lower concentrations of analytes. Fig. 9A–F shows the amperometric response obtained by successively adding analytes to a continuously stirred solutions (rotation speed 300 rpm). The insets of Fig. 9A–F showed the corresponding calibration graphs for the determination of all analytes. Such a good response of the modified electrode for oxidation of analytes studied under dynamic conditions justifies its viable application in flow systems.

3.10. Stability of the modified electrode

The PCFNiNP modified electrode showed excellent stability on continuous CV scanning. Very negligible difference was observed between the 1st and the 100th cycle of the voltammogram of the PCFNiNP modified electrode (Fig. 10) inferring that the electrode showed a good stability and the NiNP has not leached out from the modified electrode surface. The shelf-life of the modified electrode was studied over a period of 60 days at regular intervals. The modified electrode was stored in air tight container while not in use. The reproducibility of PCFNiNP modified electrode was evaluated with eight separate electrodes prepared in the similar way and the relative standard deviation was observed to be 3.2%. The stability and reproducibility of the modified electrode is attributed to the excellent immobilization procedure. This clearly demonstrates that the fabrication procedure of the modified electrode was reliable, thereby allows reproducible electroanalytical responses achieved with different sensors constructed in the similar manner. Also, the electrode was found to be reproducible after the analyte oxidation indicating that surface fouling was not observed with the modified electrode.

4. Conclusions

In summary, we have successfully fabricated the PCFNiNP modified electrode using ionic liquid as a green electrolyte. The modified electrode has been characterized using FTIR, Raman, XPS, FESEM, EDS and electrochemical techniques. The modified electrode showed excellent electrocatalytic activity for the oxidation of biologically and clinically important compounds. The proposed method has good linear range, low detection limit, and low operating potential which makes the modified electrode as a suitable electrochemical sensor for practical applications. The possibility of using this sensor in flow systems was ascertained using chronoamperometric studies.

Acknowledgments

The authors gratefully acknowledge the funding provided by the University Grants Commission (UGC), New Delhi and the Department of Science and Technology, New Delhi for financial assistance through 'PURSE' program.

References

[1] J.S. Wilkes, P. Wasserscheid, T. Welton, in: P. Asserscheid, T. Welton (Eds.), Ionic Liquids in Synthesis, Wiley-VCH, Weinheim, 2008, pp. 1–6.

[2] D. Shi, Y.M. Cao, N. Pootrakulchote, Z.H. Yi, M.F. Xu, S.M. Zakeeruddin, M. Grätzel, P. Wang, J. Phys. Chem. C 112 (2008) 17478–17485.
[3] A. Balducci, R. Dugas, P.L. Taberna, P. Simon, D. Plée, M. Mastragostino, S. Passerini, J. Power Sources 165 (2007) 922–927.
[4] R.F. de Souza, J.C. Padilha, R.S. Gonçalves, J. Dupont, Electrochem. Commun. 5 (2003) 728–731.
[5] M. Ishikawa, T. Sugimoto, M. Kikuta, E. Ishiko, M. Kono, J. Power Sources, 162 (2006) 658–662.
[6] T.-H. Tsai, S. Thiagarajan, S.-M. Chen, Electroanalysis 22 (2010) 680–687.
[7] F. Li, F. Li, J. Song, J.F. Song, D. Han, L. Niu, Electrochem. Commun. 11 (2009) 351–354.
[8] G. Jin, Y. Zhang, W. Cheng, Sens. Actuator B: Chem 107 (2005) 528–534.
[9] A.I. Gopalan, K.P. Lee, K.M. Manesh, P. Santosh, J.H. Kim, J.S. Kang, Talanta 71 (2007) 1774–1781.
[10] P. Kalimuthu, S.A. John, Talanta 80 (2010) 1086–1091.
[11] J. Mathiyarasu, S. Senthilkumar, K.L.N. Phani, V. Yegnaraman, Mater. Lett. 62 (2008) 571–573.
[12] L. Lu, X. Lin, Electrochem. Commun. 10 (2008) 704–708.
[13] S.B. Khoo, F. Chen, Anal. Chem. 74 (2002) 5734–5741.
[14] P. Shakkthivel, S.M. Chen, Biosens. Bioelectron. 22 (2007) 1680–1687.
[15] A. Liu, I. Honma, H. Zhou, Biosens. Bioelectron. 23 (2007) 74–80.
[16] S. Jiao, M. Li, C. Wang, D. Chen, B. Fang, Electrochim. Acta 52 (2007) 5939–5944.
[17] S. Senthil Kumar, S. Sriman Narayanan, Talanta 76 (2008) 54–59.
[18] A. Sivanesan, P. Kannan, S.Abraham John, Electrochim. Acta 52 (2007) 8118–8124.
[19] X. Tian, C. Cheng, H. Yuan, J. Du, D. Xiao, S. Xie, M.M.F. Choi, Talanta 93 (2012) 79–85.
[20] L. Zhang, R. Yuan, Y. Chai, X. Li, Anal. Chim. Acta 596 (2007) 99–105.
[21] A. Safavi, N. Maleki, F. Tajabadi, E. Farjami, Electrochem. Commun. 9 (2007) 1963–1968.
[22] A.N. Shipway, M. Lahav, I. Willner, Adv. Mater. 12 (2000) 993–998.
[23] L. Yang, S. Liu, Q. Zhang, F. Li, Talanta 89 (2012) 136–141.
[24] Y. Ohnuki, H. Matsuda, T. Ohsaka, N. Oyama, J. Electroanal. Chem. 158 (1983) 55–67.
[25] S. Tian, J. Liu, T. Zhu, W. Knoll, Chem. Mater. 16 (2004) 4103–4108.
[26] L. Zhang, M. Wan, J. Phys. Chem. B 107 (2003) 6748–6753.
[27] R. Davies, G.A. Schurr, P. Meenan, R.D. Nelson, H.E. Bergna, C.A.S. Brevett, R.H. Goldbaum, Adv. Mater. 10 (1998) 1264–1270.
[28] C.S.C. Bose, K. Rajeshwar, J. Electroanal. Chem. 333 (1992) 235–236.
[29] J. Li, X. Lin, Microchem. J. 87 (2007) 41–46.
[30] F. Scholz, B. Lange, Trends Anal. Chem. 11 (1992) 359–367.
[31] S.R. Krishnakumar, N. Shanthi, D.D. Sarma, Phys. Rev. B 66 (2002) 115105–115106.
[32] R. Czernuszewicz, E. Maslowsky Jr., K. Nakamoto, Inorg. Chim. Acta 40 (1980) 199–202.
[33] C.G. Munce, G.K. Parker, S.A. Holt, G.A. Hope, Coll. Surf. A, Physiochem. Eng. Aspects 295 (2007) 152–158.
[34] N. Chen, W.Q. Zhang, W.C. Yu, Y.T. Qian, Mater. Lett. 55 (2002) 230–233.
[35] T. Laibo, J.A. Lairo, J. Lukkari, Appl. Surf. Sci. 212 (2003) 525–529.
[36] G. Hu, Y. Ma, Y. Guoa, S. Shao, Electrochim. Acta 53 (2008) 6610–6615.
[37] R.-S. Schebler-Guzam, J.R. Vilche, A.J. Arvia, J. Electrochem. Soc. 125 (1978) 1578–1587.
[38] J.M. Marioli, L.E. Sereno, Electrochim. Acta 40 (1995) 983–989.
[39] R.-S. Schebler-Guzam, J.R. Vilche, A.J. Arvia, Corros. Sci. 18 (1978) 441–463.
[40] E. Laviron, J. Electroanal. Chem. 101 (1979) 19.
[41] E. Laviron, J. Electroanal. Chem. 100 (1979) 263.
[42] C.-X. Xu, K.-J. Huang, Y. Fan, Z.-W. Wu, J. Li, T. Gan, Mater. Sci. Eng., C 32 (2012) 969–974.
[43] G.-P. Jin, X. Peng, Q.-Z. Chen, Electroanalysis 20 (2008) 907–915.
[44] L. Yang, H. Xiong, X. Zhang, S. Wang, X. Zhang, Biosens. Bioelectron. 23 (2011) 3801–3805.
[45] H.-X. Wu, W.-M. Cao, Y. Li, G. Liu, Y. Wen, H.-F. Yang, S.-P. Yang, Electrochim. Acta 55 (2010) 3734–3740.
[46] W. Zhao, H. Wang, X. Qin, X. Wang, Z. Zhao, Z. Miao, L. Chen, M. Shan, Y. Fang, Q. Chen, Talanta 80 (2009) 1029–1033.
[47] C.B. McAuley, Y. Du, G.G. Wildgoose, R.G. Compton, Sens. Actuators. B: Chem. 135 (2008) 230–235.